ARTICLE



GLP-1/GIP/GCG receptor triagonist (IUB447) enhances insulin secretion via GLP-1 receptor and Gqq signalling pathway in mice

Pascale C. F. Schreier¹ · Philipp Beyerle¹ · Severin Boulassel¹ · Andreas Beck² · Aaron Novikoff^{3,4} · Peter S. Reinach⁵ · Ingrid Boekhoff¹ · Andreas Breit¹ · Arthur Neuberger¹ · Timo D. Müller^{1,3,4} · Alberto Cebrian Serrano^{3,4} · Thomas Gudermann^{1,6} · Noushafarin Khaiavi¹

Received: 20 March 2025 / Accepted: 18 June 2025 © The Author(s) 2025

Abstract

Aims/hypothesis Unimolecular peptides targeting the receptors for glucagon-like peptide-1 (GLP-1), glucose-dependent insulinotropic polypeptide (GIP) and glucagon (GCG) have been shown to improve glycaemic management in both mice and humans. Yet the identity of the downstream signalling events mediated by these peptides remain to be elucidated. Here, we aimed to assess the mechanisms by which a validated peptide triagonist for GLP-1/GIP/GCG receptors (IUB447) stimulates insulin secretion in murine pancreatic islets.

Methods Islets were isolated from wild-type (WT), Gipr-knockout ($Gipr^{-/-}$), Gcgr-knockout ($Gcgr^{-/-}$), Glp-1r (also known as Glp1r)/Gipr double-knockout and Trpm5-knockout ($Trpm5^{-/-}$) mice, followed by assessment of beta cell function and insulin secretion in response to mono- and multi-agonist administration. Metabolic phenotypes of WT and $Trpm5^{-/-}$ mice under chow and high-fat diets were investigated following triagonist application.

Results The triagonist promoted glucose-stimulated insulin secretion (GSIS) to a greater degree than co-administration of conventional mono-agonists in WT mouse islets. The triagonist-induced increase in GSIS was unchanged in the absence of either *Gipr* or *Gcgr*. However, the triagonist failed to enhance insulin secretion in islets lacking both *Glp-1r* and *Gipr* and upon treatment with the GLP-1 receptor-specific antagonist exendin-3 (9–39). Similarly, the specific blocking of Gαq signalling with YM254890 or transient receptor potential melastatin 5 (TRPM5) with triphenylphosphine oxide (TPPO) suppressed the triagonist-induced enhancement of GSIS. In vivo assessment of high-fat-fed *Trpm5*^{-/-} mice demonstrated the absence of triagonist-induced therapeutic effects on glycaemic management.

Conclusions/interpretation Triagonist-induced augmentation of GSIS is primarily mediated through its interaction with the GLP-1 receptor and subsequent activation of the $G\alpha q$ -TRPM5 signalling pathway. Given that $G\alpha q$ is a key player in the amplification of GSIS, particularly under diabetic conditions, these findings highlight a GLP-1 receptor-centric pharmacological profile that underlies the potent effects of this multi-receptor agonist.

Keywords GLP-1 receptor · Gαq signalling · Insulin secretion · Pancreatic islet · Triagonist · TRPM5

- Noushafarin Khajavi Noushafarin.Khajavi@lrz.uni-muenchen.de
- ☐ Thomas Gudermann
 Thomas.Gudermann@lrz.uni-muenchen.de

Published online: 09 September 2025

- Walther Straub Institute of Pharmacology and Toxicology, LMU Munich, Munich, Germany
- Institute of Experimental and Clinical Pharmacology and Toxicology, Saarland University, Homburg, Germany
- ³ Institute of Diabetes and Obesity, Helmholtz Munich, Munich, Germany
- German Center for Diabetes Research (DZD), Neuherberg, Germany
- Wenzhou Medical University, Ophthalmology Department, Wenzhou, P. R. China
- ⁶ German Center for Lung Research (DZL), Munich, Germany



Research in context

What is already known about this subject?

- GLP-1, glucagon and GIP are three distinct hormones with unique roles that contribute to glucose homeostasis
- A rationally designed unimolecular GLP-1/GIP/glucagon receptor triagonist (IUB447) has exhibited superior glycaemic efficacy over existing dual agonists and best-in-class mono-agonists in rodent models
- The contribution of each receptor to the insulinotropic response elicited by the triagonist, as well as the possibility of unique ligand structure-function interactions, remains unexplored

What is the key question?

Does the GLP-1/GIP/glucagon receptor triagonist uniquely engage the beta cell insulinotropic response?

What are the new findings?

- The triagonist augments cytosolic Ca²⁺ magnitudes induced by high glucose concentrations and elicits greater glucose-stimulated insulin secretion (GSIS) compared with the co-administration of conventional mono-agonists in murine islets
- The triagonist-driven augmentation of GSIS was not diminished by the absence of either GIP or glucagon receptors
- The insulinotropic action of the triagonist is primarily mediated through the GLP-1 receptor and subsequent activation of the Gaq-TRPM5 signalling cascade

How might this impact on clinical practice in the foreseeable future?

Our findings highlight a GLP-1 receptor-centric mechanism underlying the potent pharmacological effects of this multi-receptor agonist and underscore the therapeutic potential of selectively targeting the Gag-TRPM5 signalling pathway as a novel strategy for mitigating T2D pathophysiology

Abbreviations	
$[Ca^{2+}]_i$	Intracellular Ca ²⁺ concentration
ER	Endoplasmic reticulum
GCG	Glucagon
GCGR	Glucagon receptor
GIP	Glucose-dependent insulinotropic polypeptide
GIPR	Glucose-dependent insulinotropic polypeptide
	receptor
GLP-1	Glucagon-like peptide-1
GLP-1R	Glucagon-like peptide-1 receptor
GSIS	Glucose-stimulated insulin secretion
HFD	High-fat diet
LFD	Normal chow diet
KO	Knockout

Phospholipase C **TPPO** Triphenylphosphine oxide

Protein kinase C

Nucleotide

TRPM5 Transient receptor potential melastatin 5

WT Wild-type

Introduction

Combinational pharmacotherapies provide a promising approach for the treatment of obesity and type 2 diabetes. Co-agonism, or tri-agonism, of separate therapeutic targets leverage strategic combinatorial synergism to amplify satiety, body-weight lowering and glucoregulatory benefits. Previous studies demonstrate that sequence hybridisation of glucagon-like peptide-1 (GLP-1), glucose-dependent insulinotropic polypeptide (GIP) and glucagon (GCG) into a unimolecular triple agonist (GLP-1/GIP/GCG) effectively enhances glycaemic management relative to conventional mono-agonist treatments in diet-induced obese mice [1, 2]. These desirable effects are prompting efforts to clarify the identity of signalling pathway mechanisms that mediate such responses in health and disease.

Long-acting GLP-1 receptor (GLP-1R) mono-agonists have been developed to engage in beta cell glucosedependent insulinotropic effect, while also acting within key feeding regions of the central nervous system to



nt

PKC

PLC

influence satiety. GCG is primarily known for its essential role in maintaining glucose homeostasis through its activation of hepatic glycogenolysis and gluconeogenesis during periods of starvation [3]. However, long-acting GCG receptor (GCGR) agonists have also been shown to dose-dependently stimulate insulin secretion and enhance energy expenditure and fatty acid oxidation, leading to substantial weight loss in rodents [4, 5]. These findings led to the strategic development of a unimolecular GLP-1/ GCG co-agonist that exploits the energy expenditure and lipolytic properties of GCG and the appetite-suppressing and insulinotropic properties of GLP-1 [6]. A cautionary note on GLP-1-based pharmacology is the limitation on dose escalation due to corresponding increases in gastrointestinal tolerability issues. To mitigate this drawback, the pharmacological administration of GIP, primarily known for its insulinotropic and mild appetite-suppressing properties [7], is also suggested to have an anti-emetic effect, potentially allowing GIP co-agonism to increase tolerability to the GLP-1 component [8].

The complementary nature of the desirable attributes in GLP-1, GIP and GCG led to the creation of a unimolecular hybridised triagonist with retained and balanced activity across the GLP-1R, GIP receptor (GIPR) and GCGR [1]. Despite definitive evidence suggesting that the triagonist offers a promising therapeutic option for the treatment of type 2 diabetes, the specific cellular mechanism by which the enhanced efficacy in glycaemic management is attained remains unclear.

The GLP-1R/GIPR/GCGR triagonist IUB447 enhances glycaemic management through concurrent activation of GLP-1R, GIPR and GCGR, and corresponds to the triagonist previously reported by Finan et al [1]. Recently, we found that triagonist-induced enhancement of insulin secretion exceeds levels observed with the loose co-administration of the three individual agonists in murine islets [9]. This difference raises the first question: does the superior triagonist effect stem from an additional mode of action beyond the activation of the three receptors?

Accumulating evidence suggests that GLP-1R activates both G α q and G α s signalling pathways, whereas GIPR and GCGR primarily couple to G α s [10–12]. Under diabetic conditions, persistent beta cell depolarisation shifts GLP-1R signalling toward G α q dominance, preserving its insulinotropic effect [13]. This shift may account for why GLP-1R agonists remain a useful glucose-lowering therapy, whereas GIPR loses insulinotropic efficacy [13–15]. Given the potential loss of effectiveness in G α s signalling in diabetic conditions and that both GIP and GCG seem to primarily act through G α s signalling, it raises a second question: is the effect of triagonist on glucose-stimulated insulin secretion (GSIS) mediated solely via GLP-1R?

In this study, we sought to unravel the mechanisms through which the triagonist enhances insulin secretion in murine islets.

Methods

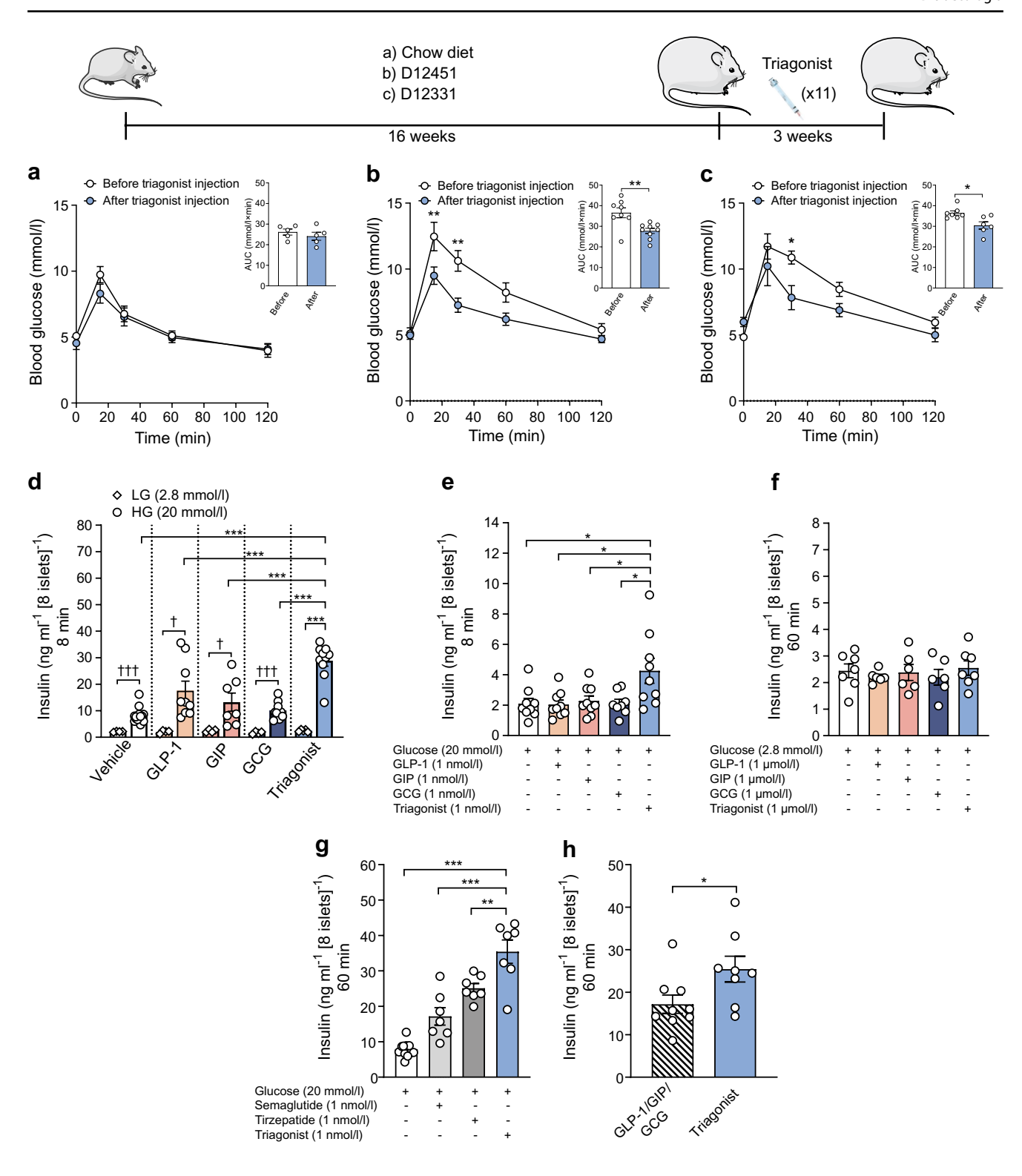
The sources of reagents are listed in electronic supplementary material (ESM) Table 1.

Mouse strains $Gipr^{-/-}$, $Gcgr^{-/-}$ and Glp-1r (also known as Glp1r)/Gipr double-knockout (KO) mice were generated. sgRNAs against exons 4 and 5 of the Gipr, Glp-1r and Gcgr genes (ESM Table 2) were designed using CRISPOR tool (www.crispor.tefor.net), in vitro transcribed (E3322, NEB) and purified using the MEGAclear Kit. C57BL/6n female mice at 4 weeks of age were super ovulated and mated with C57BL/6n studs. Fertilised oocytes were electroporated (NEPA21) with a total concentration of 200 ng/µl sgR-NAs and 200 ng/µl recombinant NLS-Cas9 protein. Electroporated zygotes were surgically implanted into recipient CD1 females. For genotyping, ear biopsies were lysed and genomic DNA was purified. Target genes were amplified using primers listed in ESM Table 3 and verified by Sanger sequencing to confirm CRISPR-induced deletions. Founders carrying the following deletion alleles were bred to generate single and double KO lines: a five-nucleotide (nt) deletion in exon 5 of Gipr; a 62-nt deletion in exon 4 of Gcgr; and a 495-nt deletion spanning exon 4, intron 4 and exon 5 of Glp-1r. CRISPR-Cas9-induced deletions result in a premature stop codon at the exon 5 (Gipr and Gcgr) and 6 (Glp-1r). To genotype the Gipr deletion, specific primers binding on the wild-type (WT) or deleted DNA region were designed and established (Gipr-9-nt forward and reverse, and Gipr WT reverse primers) (ESM Table 3). Gcgr and Glp-1r deletions were genotyped by PCR and resolved on agarose gel electrophoresis until double bands were obtained.

Transient receptor potential melastatin 5 (TRPM5) KO (B6;129-*Trpm*5tm1Csz/J) mice were obtained from Jackson Laboratory (https://www.jax.org/strain/013068). Heterozygous *Trpm5*^{+/-} mice were bred to obtain age- and sexmatched homozygous wild-type (WT) and homozygous *Trpm5*^{-/-} mice. Genotyping was performed using the One Step Mouse Genotyping Kit. *Trpm5* transgene inheritance was confirmed by PCR (primers in ESM Table 3; protocol in ESM Table 4).

Mice were fed a normal chow diet (LFD) or a highfat diet (HFD) (D12451 or D12331), with 45% and 58% energy from fat, respectively. After being fed the HFD for 16 weeks, mice were treated every other day with either vehicle or triagonist (3 nmol/kg) for 3 weeks. Mice were single- or group-housed under a 12 h light-dark cycle at





22°C with ad libitum access to food and water. Mice were randomly assigned to experimental groups using a random number generator. This ensured unbiased allocation and reduced potential confounding factors. Experimenters were masked to group assignments during outcome assessment

to minimise bias. No animals, samples, or data points were excluded from the analysis. All experiments complied with the EU Animal Welfare Act and were approved by the District Government of Upper Bavaria, Germany (permit no. 55.2–2532. Vet_02-21-75).



∢Fig. 1 Triagonist improves glucose metabolism and GSIS in mice. (a-c) Ten- to twelve-week-old WT C57BL/6 mice were divided into three groups and assigned to different diets. A GTT was performed before and after 3 weeks of treatment with 3 nmol/kg triagonist given by i.p. injection every other day. (a-c) One group was maintained on chow diet (LFD) (n=7) (a), while the other two groups were placed on different HFDs, either D12451 (b) or D12331 (c), for 16 weeks $(n \ge 7 \text{ per group})$. For the GTT, mice were fasted overnight. Blood glucose levels (mmol/l) before and within 2 h after i.p. injection of glucose (2 g/kg body weight) are shown, together with the AUC for glucose (in mmol/ $1 \times min$). (d, e) Insulin secretion (ng ml⁻¹ [8 islets]⁻¹) was assessed in isolated islets from WT mice on LFD ($n \ge 3$ mice, measured in duplicate). After 1 h pre-incubation in KRB with 2.8 mmol/l glucose, islets were stimulated with 2.8 mmol/l glucose (LG) or 20 mmol/l glucose (HG) supplemented with mono- or multiagonist (1 nmol/l each). Insulin content was determined, by ELISA, in supernatant fractions collected at 60 min (d) or 8 min (e) after stimulation. (f) Insulin secretion was assessed following 1 h stimulation with a glucose concentration of 2.8 mmol/l, supplemented with mono- or multi-agonist (1 µmol/l each). (g) Insulin secretion was assessed following 1 h stimulation with glucose 20 mmol/l, supplemented with the glucose-lowering drugs semaglutide (1 nmol/l) or tirzepatide (1 nmol/l), in comparison with the response elicited by the triagonist (1 nmol/l). (h) Insulin secretion was assessed following 1 h stimulation with 20 mmol/l glucose, supplemented with either a triagonist or co-administration of mono-agonists (1 nmol/l each). Data show means \pm SEM, and statistical differences were assessed by twoway ANOVA (a-c, blood glucose), unpaired two-tailed Student's t test (a-c, AUC for glucose; h) or one-way ANOVA (d-g). Circles in bar graphs represent single values. *p<0.05; **p<0.01; ***p<0.001 for indicated comparisons; †p<0.05, †††p<0.001 for HG vs LG

Characterisation of glucose homeostasis GTTs were performed as previously described [16]. Mice were fasted for 16 h and injected intraperitoneally with glucose (2 g/kg body weight). Blood glucose was measured using a glucometer (TheraSense FreeStyle) at 0, 15, 30, 60 and 120 min. Plasma was collected post-euthanasia, stored at -80°C, and analysed for insulin and GCG levels by ELISA.

Islet isolation and determination of insulin secretion Islet isolation was performed as previously described [9]. In brief, the pancreas was perfused via the common bile duct with collagenase-P (0.3 mg/ml). Isolated islets were cultured for 48 h in RPMI 1640 before use in functional assays. For GSIS, islets were equilibrated for 1 h in KRB buffer (ESM Table 5) with 2.8 mmol/l glucose. Next, islets were incubated for 1 h in 20 mmol/l glucose supplemented with agonists in the presence or absence of blockers. Exendin-3 (GLP-1 blocker), LY2409021 (GCG blocker), YM-254890 (G α q blocker), MDL-12330A (adenylate cyclase blocker), calphostin C (protein kinase C [PKC] blocker) and TPPO (TRPM5 blocker) were used as specific inhibitors. Insulin was quantified in the supernatant fraction using ELISA.

Cell culture MIN6 cells were provided by P.-O. Berggren and B. Leibiger, Karolinska Institutet, Stockholm, Sweden. Cells were cultured at 37°C with 5% CO_2 in DMEM supplemented with 10% FBS, 100 U/ml penicillin, 100 μ g/ml streptomycin and 75 μ mol/l β -mercaptoethanol. The cells were routinely tested and no mycoplasma contamination was detected. Authentication of the MIN6 cell line was performed based on morphology and functional characteristics.

Calcium imaging Changes in intracellular Ca^{2+} concentration ($[Ca^{2+}]_i$) were recorded as previously described [17]. Confocal imaging was performed using a Zeiss LSM 510 Meta system with a 63×/NA1.2 water immersion objective. Regions of interest were selected using LSM software, and calcium dynamics were monitored via Fluo-4 fluorescence (excitation λ : 488 nm; emission λ : 500–550 nm). Images (8-bit, 512 × 512 pixels) were acquired every 5 s.

α Screen-based detection of intracellular cAMP Islets were plated in clear-bottom 96-well plates with KRB containing 2.8 mmol/l glucose and stimulated for 20 min at 37°C with KRB (20 mmol/l glucose) plus IBMX (500 μmol/l), either alone or combined with forskolin (10 μmol/l), GLP-1 (1 nmol/l) or triagonist (1 nmol/l). Stimulation was terminated by adding lysis buffer containing acceptor beads and biotinylated cAMP. After 90 min, donor beads were added and incubated for 60 min. Acceptor bead emission (λ 570 ± 100 nm) was measured after donor bead excitation (λ 680 ± 40 nm) using a ClarioStar plate reader (BMG, Offenburg, Germany).

Morphological analysis Islet morphology was assessed by H&E staining of 10 μm cryosections and whole-islet immunofluorescence. Antibodies are shown in ESM Table 6; antibody validation was carried out according to the manufacturers' specifications, and all relevant information, including recommended dilutions and buffer compositions, was provided by the manufacturers. Imaging was done using a Meta-Systems scanner with a Zeiss Imager Z.2 microscope, and quantitative analysis with FIJI 2.16.0 [18].

Statistics Data were expressed as mean \pm SEM. A p value less than 0.05 was considered significant. Graphical presentations and statistics were obtained by Prism software (version 9.0.1; GraphPad). For comparison of two groups, p values were calculated by the unpaired two-tailed Student's t test for parametric distribution or Mann–Whitney test for non-parametric distribution. For three or more groups, one-way ANOVA with Bonferroni multiple comparison were used for parametrically distributed data. Glucose tolerance tests were compared using two-way ANOVA with Bonferroni multiple comparison.



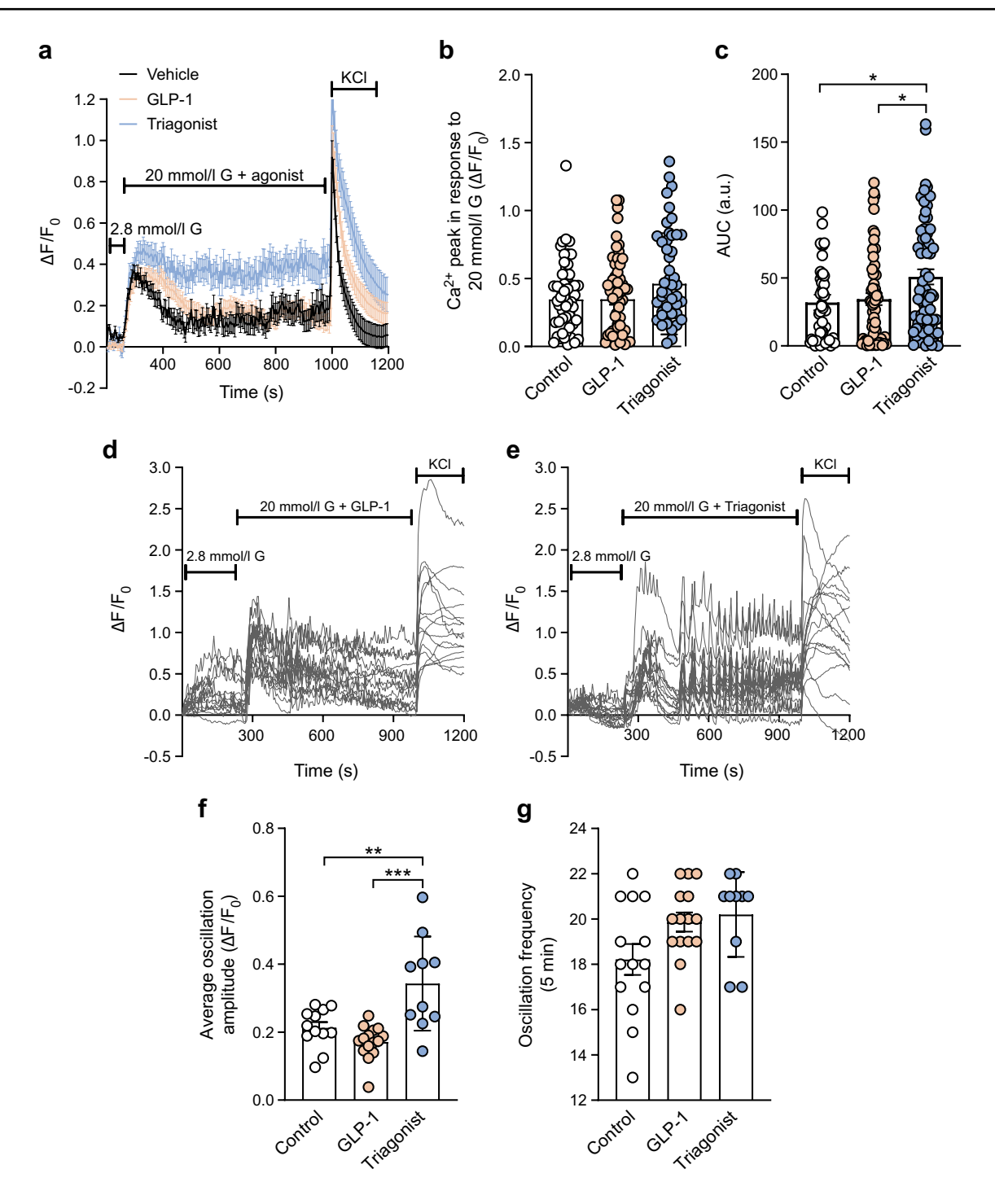


Fig. 2 Triagonist increases cytoplasmic Ca^{2+} concentration in beta cells. (a) Intact WT islets ($n \ge 50$ islets per condition, isolated from at least ten mice) were loaded with 3 µmol/l Fluo-4-AM and alterations in $[Ca^{2+}]_i$ of individual cells were monitored by confocal microscopy after increasing the extracellular glucose concentration from 2.8 to 20 mmol/l in the presence of GLP-1 (1 nmol/l) or triagonist (1 nmol/l). KCl (30 mmol/l) was used as a positive control. F_0 was calculated as the mean fluorescence intensity during the final 2 min prior to stimulation with glucose 20 mmol/l + agonist to minimise potential bias from differences in dye loading, photobleaching or probe stabilisation. (b, c) Average of Ca^{2+} influx peaks assessed from baseline after glucose stimulation (b) and AUC (only during agonist application, c).

(**d**, **e**) Individual traces of Fluo-4 intensity of single islet cells in the presence of GLP-1 (1 nmol/l, **d**) or triagonist (1 nmol/l, **e**), elicited by excitation at λ 480 nm (indicative of $[Ca^{2+}]_i$). (**f**) Average $[Ca^{2+}]_i$ oscillation amplitude calculated based on alteration in Fluo-4 intensity in single cells following an initial peak after 20 mmol/l glucose stimulation or in the presence of different agonists ($n \ge 10$ cells). (**g**) Representative changes in frequency of $[Ca^{2+}]_i$ oscillations in 5 min following an initial peak after 20 mmol/l glucose stimulation or in the presence of different agonists ($n \ge 10$ cells). The data are presented as means \pm SEM (circles in bar graphs represent single values) and statistical differences were assessed by one-way ANOVA (**b**, **c**, **f**, **g**). *p < 0.05, **p < 0.01, ***p < 0.01. a.u., arbitrary units; G, glucose



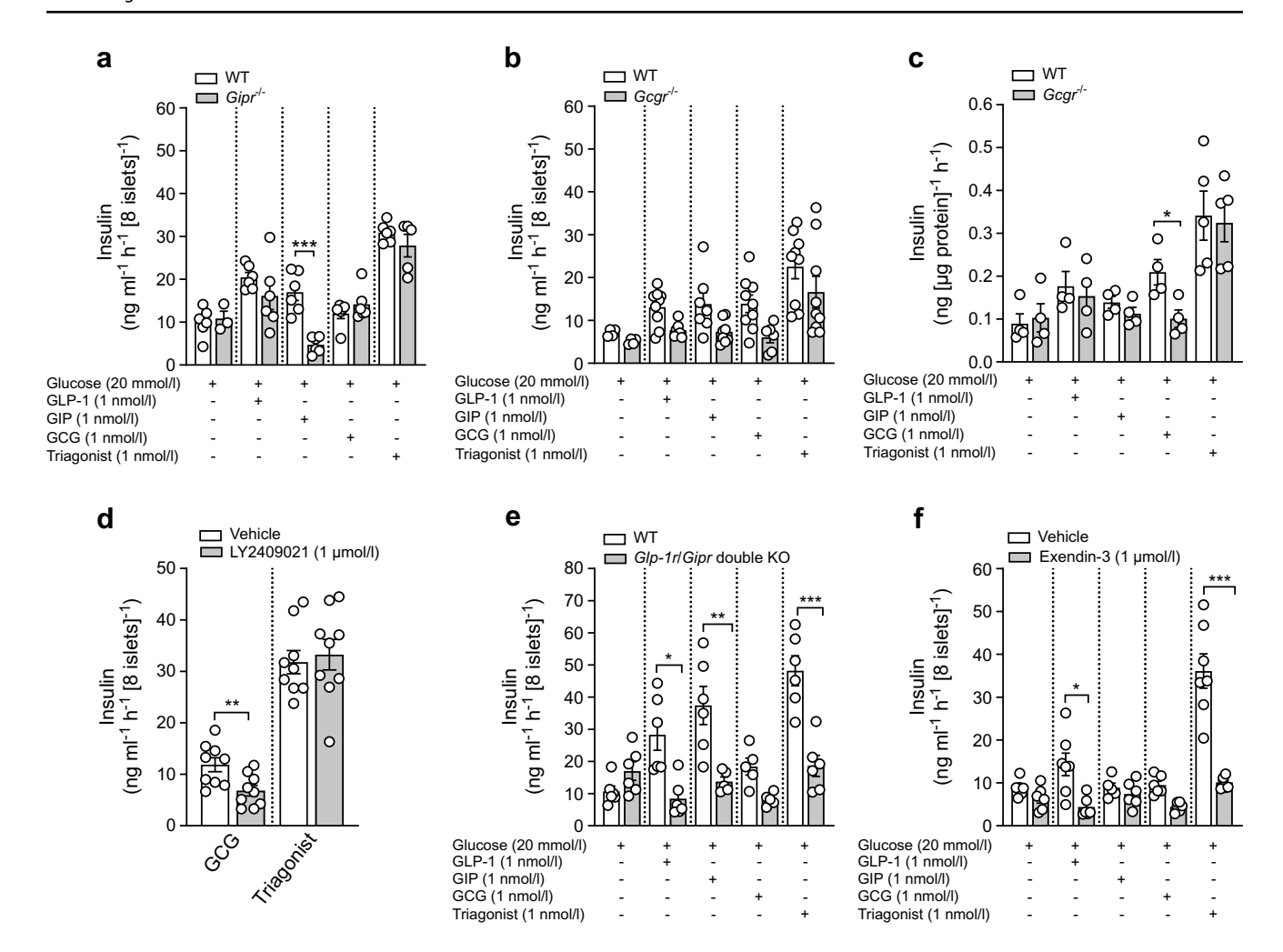


Fig. 3 Triagonist primarily enhances GSIS through activation of the GLP-1R. Insulin secretion was assessed after 1 h pre-incubation in KRB with 2.8 mmol/l glucose; islets were stimulated with 20 mmol/l glucose, supplemented with mono- or multi-agonist (1 nmol/l each). (**a**, **b**) Insulin secretion (ng ml⁻¹ h⁻¹ [8 islets]⁻¹) in isolated islets from WT mice vs either $Gipr^{-/-}$ mice (**a**) or $Gcgr^{-/-}$ mice (**b**) on a chow diet (LFD) ($n \ge 3$ mice per condition). (**c**) Insulin secretion normalised to protein content (ng [µg protein]⁻¹ h⁻¹) in isolated islets from WT and $Gcgr^{-/-}$ mice on LFD ($n \ge 4$ mice per condition). (**d**) Insulin secretion (ng ml⁻¹ h⁻¹ [8 islets]⁻¹) in isolated islets from WT mice on LFD ($n \ge 5$ mice per condition) after 1 h pre-incubation in KRB with 2.8 mmol/l glucose in the presence or absence of 1 µmol/l LY2409021. Islets were stimulated with 20 mmol/l glucose

 \pm blocker, supplemented with GCG or triagonist (1 nmol/l each). (e) Insulin secretion (ng ml⁻¹ h⁻¹ [8 islets]⁻¹) in isolated islets from WT, *Glp-1r/Gipr* double KO mice on LFD ($n \ge 3$ mice per condition). (f) Insulin secretion (ng ml⁻¹ h⁻¹ [8 islets]⁻¹) in isolated islets from WT mice on LFD ($n \ge 5$ mice per condition) after 1 h pre-incubation in KRB with 2.8 mmol/l glucose in the presence or absence of 1 µmol/l exendin-3. Islets were stimulated with 20 mmol/l glucose \pm blocker, supplemented with mono- or multi-agonist (1 nmol/l each). Insulin content in supernatant fractions were collected 60 min after stimulation and ELISA was used to determine the insulin content in the fraction. The data are presented as means \pm SEM (circles in bar graphs represent single values) and statistical differences were assessed by unpaired two-tailed Student's t test. *p < 0.05, **p < 0.01, ***p < 0.001

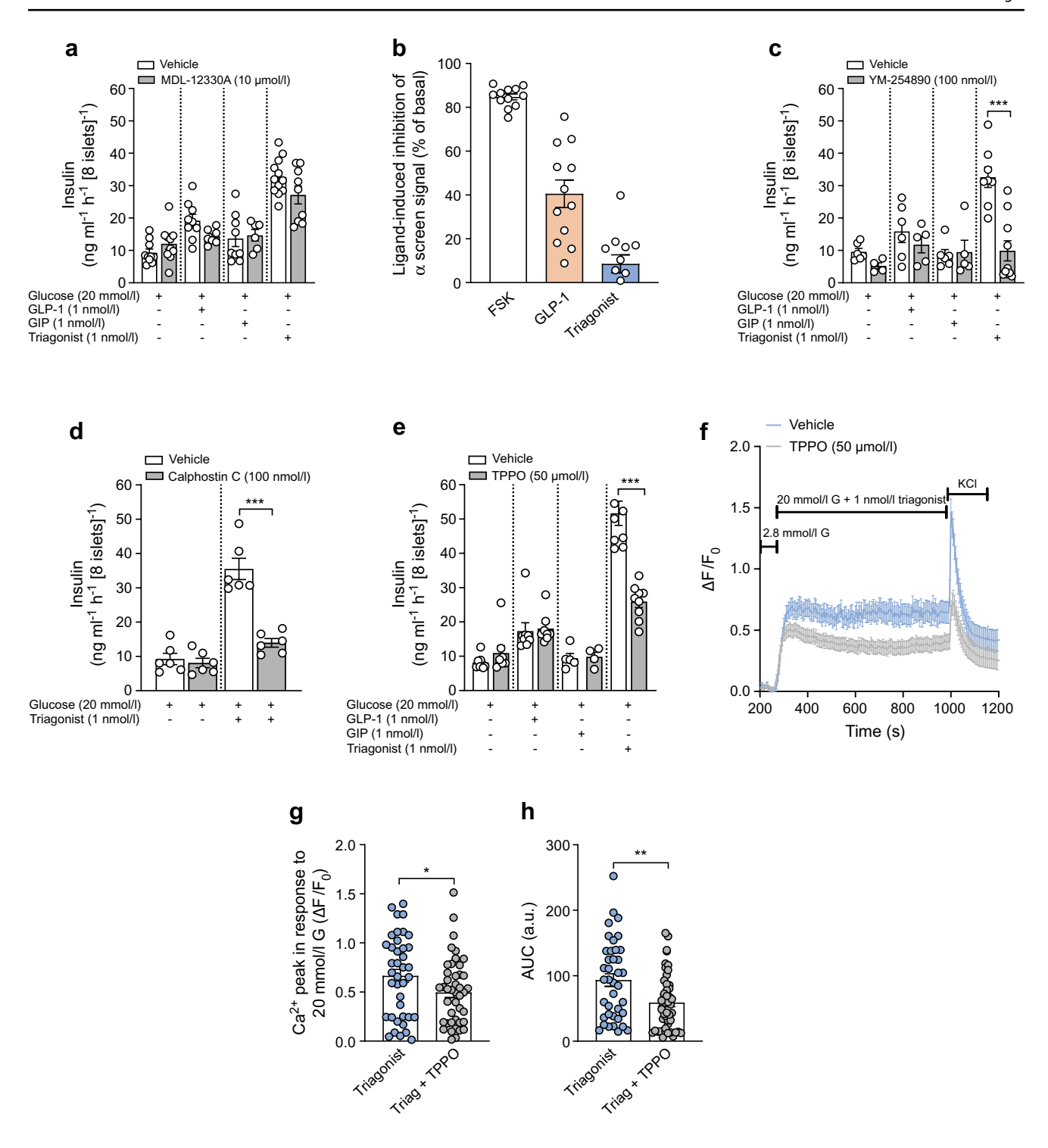
Results

Triagonist effectively reverses glucose metabolism dysfunction induced by HFD in WT mice Ten- to twelve-week-old WT (C57BL/6) mice were fed LFD or obesogenic diets (D12451 or D12331) for 16 weeks. Triagonist-induced improvements in glucose tolerance were assessed relative to pre-treatment levels within each diet group. Both HFDs markedly impaired glucose tolerance (ESM Fig. 1a, b). Three weeks of the triagonist treatment improved glucose

tolerance in HFD-fed mice, with minimal effect in LFD-fed controls (Fig. 1a-c).

Triagonist increases GSIS in primary islets To assess the effects of the triagonist and mono-agonists on GSIS, single islets from WT mice fed an LFD were exposed to a switch from low glucose (2.8 mmol/l) to high glucose (20 mmol/l), with or without agonists. Supernatant fractions were collected at 8 and 60 min. The glucose switch alone induced a ~fourfold increase in insulin secretion after 60 min; GLP-1,





GIP and GCG (each at 1 nmol/l) enhanced GSIS by ~eightfold, ~fivefold and ~fourfold, respectively, whereas the triagonist (1 nmol/l) elicited an ~11-fold increase (Fig. 1d). Notably, after 8 min, only the triagonist significantly increased GSIS (~twofold), with the mono-agonists having no effect (Fig. 1e). Elevating the concentration of triagonist to 1 μmol/l had no effect on insulin secretion at a glucose concentration of 2.8 mmol/l (Fig. 1f), ruling out potential

islet-derived hypoglycaemia and reinforces glucose-dependency as a mode of action. The triagonist similarly enhanced GSIS in MIN6 cells, excluding alpha cell-derived GCG as underlying mechanism of its superior effect (ESM Fig. 2a). The stimulatory effect of triagonist on GSIS surpassed that of the two glucose-lowering drugs, semaglutide and tirzepatide, in WT mouse islets (Fig. 1g). Triagonist-enhanced GSIS was up to 50% greater than that seen with semaglutide



∢Fig. 4 Triagonist improves GSIS in isolated islets through Gαq signalling and TRPM5 activation. (a) Insulin secretion (ng ml⁻¹ h⁻¹ [8 islets]⁻¹) in isolated islets from WT mice on a chow diet (LFD) $(n \ge 5 \text{ mice per condition, measured in duplicate})$. After 1 h pre-incubation in KRB with 2.8 mmol/l glucose in the presence or absence of 10 µmol/l MDL-12330A, islets were stimulated with 20 mmol/l glucose ± blocker, supplemented with mono- or multi-agonist (1 nmol/l each). Insulin content was determined by ELISA in supernatant fractions collected 60 min after stimulation. (b) Inhibition of cAMP-dependent α screen signals is shown after stimulation of islets with 10 umol/l forskolin, 1 nmol/l GLP-1 or 1 nmol/l triagonist for 20 min at 37°C. Data from four independent experiments performed in triplicate are presented as mean \pm SEM of ligand-induced inhibition of the α screen signal as % of basal. (c-e) Insulin secretion (ng ml⁻¹ h^{-1} [8 islets]⁻¹) in isolated islets from WT mice on LFD (*n*≥5 mice per condition, measured in duplicate) in the presence or absence of 100 nmol/l YM-254890, 100 nmol/l calphostin C or 50 µmol/l TPPO. (f) Intact islets from WT mice $(n \ge 38 \text{ cells per condition, isolated})$ from at least eight mice) were loaded with 3 µmol/l Fluo-4-AM and alterations in [Ca2+]i of individual cells were monitored by confocal microscopy after increasing the extracellular glucose concentration from 2.8 to 20 mmol/l in the presence of triagonist (1 nmol/l) with (grey) or without (blue) 50 µmol/l TPPO. KCl (30 mmol/l) was used as a positive control. F₀ was calculated as the mean fluorescence intensity during the final 2 min prior to stimulation with 20 mmol/l glucose + agonist. (\mathbf{g}, \mathbf{h}) Average of Ca^{2+} influx peaks assessed from baseline after glucose stimulation (g) and AUC (only during agonist application [h]). The data are presented as means \pm SEM (circles in bar graphs represent single values) and statistical differences were assessed by unpaired two-tailed Student's t test (a, c, d, e, g, h). *p<0.05, **p<0.01, ***p<0.001. a.u., arbitrary units; FSK, forskolin; G, glucose; Triag, triagonist

and 25% greater than that seen with tirzepatide. Surprisingly, the triagonist increased GSIS by up to 35% compared with loose co-administration of GLP-1, GIP and GCG, in both mouse islets and MIN6 cells (Fig. 1h and ESM Fig. 2b).

Triagonist enhances cytosolic Ca²⁺ responses induced by high glucose We next examined whether triagonist-enhanced GSIS is associated with increased Ca²⁺ mobilisation in beta cells. At 2.8 mmol/l glucose, beta cells exhibited low and relatively stable [Ca²⁺]_i levels, whereas 20 mmol/l glucose triggered transient Ca²⁺ increases, combined with frequent oscillatory patterns (Fig. 2a). The initial Ca²⁺ peak following glucose stimulation was comparable across control (vehicle), GLP-1 (1 nmol/l) and triagonist (1 nmol/l) (Fig. 2b). After cessation of Ca²⁺ transient activity, [Ca²⁺] remained elevated with the triagonist compared with control and GLP-1 (Fig. 2c). Notably, the amplitude of oscillations during the plateau phase was significantly higher with triagonist treatment (Fig. 2d–f), whereas oscillation frequency was only slightly increased with GLP-1 and triagonist relative to control (Fig. 2g).

Triagonist enhances GSIS mainly through GLP-1R activation Next, we assessed the relative contribution made by GLP-1R, GIPR and GCGR towards mediating triagonistinduced responses. Accordingly, triagonist-induced GSIS was evaluated in islets from Gipr^{-/-}, Gcgr^{-/-}, and Glp-1r/ Gipr double KO mice, compared with their WT controls. The triagonist-induced augmentation of GSIS was comparable between $Gipr^{-/-}$ and WT mouse islets (Fig. 3a). A modest reduction in triagonist-induced insulin secretion was observed in $Gcgr^{-/-}$ islets (Fig. 3b). Notably, a similar reduction in insulin secretion was observed in response to other secretagogues in $Gcgr^{-/-}$ mouse islets. To rule out technical artefacts, we evaluated mono- and multi-agonist effects on GSIS in Gcgr^{-/-} and control mice, normalising insulin secretion to protein content. GCG-induced GSIS was significantly reduced in Gcgr^{-/-} mouse islets, whereas GLP-1-, GIP- and triagonist-induced insulin secretion remained comparable with insulin secretion in WT mice (Fig. 3c). Furthermore, the selective GCGR antagonist LY2409021 (1 µmol/l) effectively suppressed GCG-induced insulin secretion but had no impact on the triagonist-enhanced GSIS in WT islets (Fig. 3d). Surprisingly, the triagonist-induced augmentation of GSIS was completely abolished in Glp-1r/Gipr double KO islets (Fig. 3e). A similar response was obtained in WT islets treated with the GLP-1R antagonist exendin-3; at 1 µmol/l, exendin-3 suppressed triagonist-induced insulin secretion by up to 70% (Fig. 3f).

Triagonist enhances GSIS primarily through the Gag-TRPM5 signalling pathway GLP-1R activation is known to engage both $G\alpha s$ and $G\alpha q$ signalling pathways. We next assessed their relative contributions towards triagonist-induced GSIS. The adenylate cyclase inhibitor MDL-12330A (10 µmol/l) caused only a modest reduction in GSIS responses to GLP-1 and triagonist in islets from WT mice fed an LFD (Fig. 4a). Next, we measured intracellular cAMP in WT mouse islets using an α screen assay to assess G α s activation. The adenylate cyclase activator forskolin increased cAMP-dependent signals by over 80% relative to baseline (Fig. 4b). GLP-1 (1 nmol/l) raised cAMP levels by about 40%, whereas the triagonist did not significantly increase cAMP above baseline, suggesting that Gas signalling may not be the primary pathway mediating triagonist-induced GSIS.

Next, we examined the role of $G\alpha q$ signalling in triagonist-induced GSIS. Inhibition of $G\alpha q$ with 100 nmol/l YM-254890 had no significant effect on GLP-1- or GIP-induced GSIS in islets from WT mice fed LFD (Fig. 4c). Notably, YM-254890 reduced triagonist-induced GSIS by up to 70% (Fig. 4c). It is worth noting that both GLP-1 and GIP elicited only modest insulin secretion, and the inhibitory effects of adenylate cyclase and $G\alpha q$ blockers were not particularly pronounced. We believe these results are due to the nanomolar agonist concentrations applied, which were selected to simulate receptor activation levels similar to those that might occur physiologically, even if not precisely matching actual in vivo concentrations.



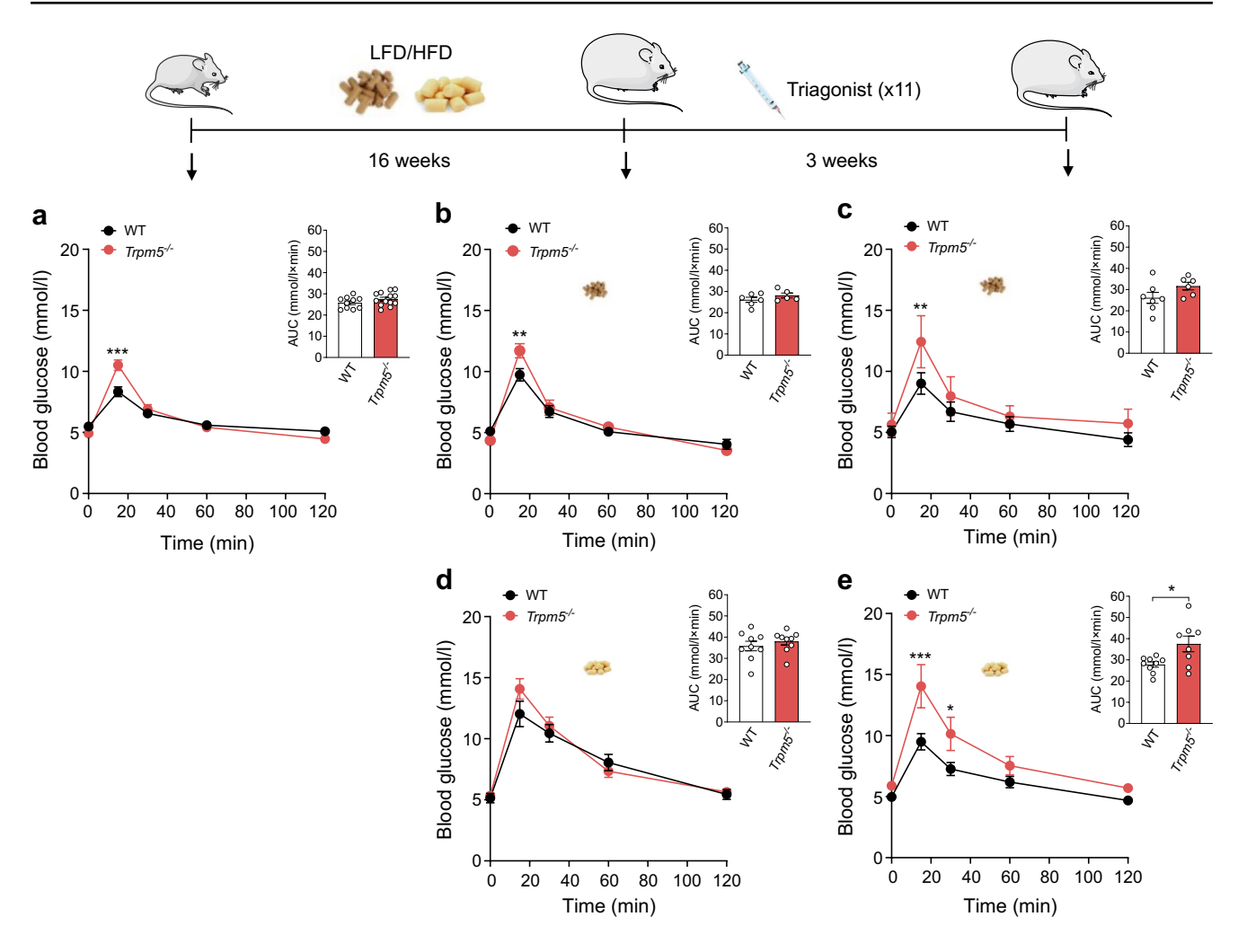


Fig. 5 TRPM5 plays a crucial role in mediating the beneficial effects of triagonist on glucose metabolism in mice fed HFD. Ten- to twelve-week-old WT or $Trpm5^{-/-}$ mice were divided into two groups: one maintained on a normal chow (LFD) $(n \ge 6)$; and the other on D12451 (HFD) diet for 16 weeks $(n \ge 9)$. Following 16 weeks of the respective diets, both groups received an i.p. injection of 3 nmol/kg triagonist every other day for 3 weeks (11 injections); GTT was performed before (**a**) and after the LFD (**b**) or HFD (**d**) and after the triagonist

treatment in the LFD (c) and HFD (e) groups. For the GTT, mice were fasted overnight. Blood glucose levels before and within 2 h after i.p. injection of glucose (2 g/kg of body weight) in WT (black) and $Trpm5^{-/-}$ mice (red) are shown, together with the corresponding AUC. Data show means \pm SEM, and statistical differences were assessed by two-way ANOVA (blood glucose) or unpaired two-tailed Student's t test (glucose AUC). Circles in bar graphs represent single values. *p<0.05, **p<0.01, ***p<0.001

Given that PKC and TRPM5 are downstream effectors of $G\alpha q$ signalling in beta cells, our next step involved determining whether the PKC inhibitor (calphostin C) and TRPM5 blocker (TPPO) suppress the triagonist-induced increase in GSIS. We demonstrated that 100 nmol/l calphostin C and 50 μ mol/l TPPO each reduced the triagonist-induced GSIS increase by about 60% in primary islets (Fig. 4d, e). Next, we evaluated the impact of TPPO on triagonist-induced Ca^{2+} signalling in beta cells (Fig. 4f–h). TPPO significantly reduced the initial Ca^{2+} peaks induced by 20 mmol/l glucose in the presence of the triagonist and attenuated the sustained intracellular Ca^{2+} elevation in intact islets (Fig. 4g,

h). Notably, the triagonist had no impact on [Ca²⁺] in the absence of extracellular Ca²⁺ (ESM Fig. 3). Nonetheless, Ca²⁺ release in response to the sarcoplasmic/endoplasmic reticulum (ER) calcium ATPase (SERCA) pump blocker cyclopiazonic acid demonstrated the sheer availability of ER calcium, ruling out the role of ER calcium in triagonist-induced Ca²⁺ signalling in beta cells.

Dependence of triagonist-enhanced glycaemic effects on TRPM5 function To confirm that the therapeutic effects of the triagonist depend on TRPM5 function, we assessed whether its beneficial effects were diminished in



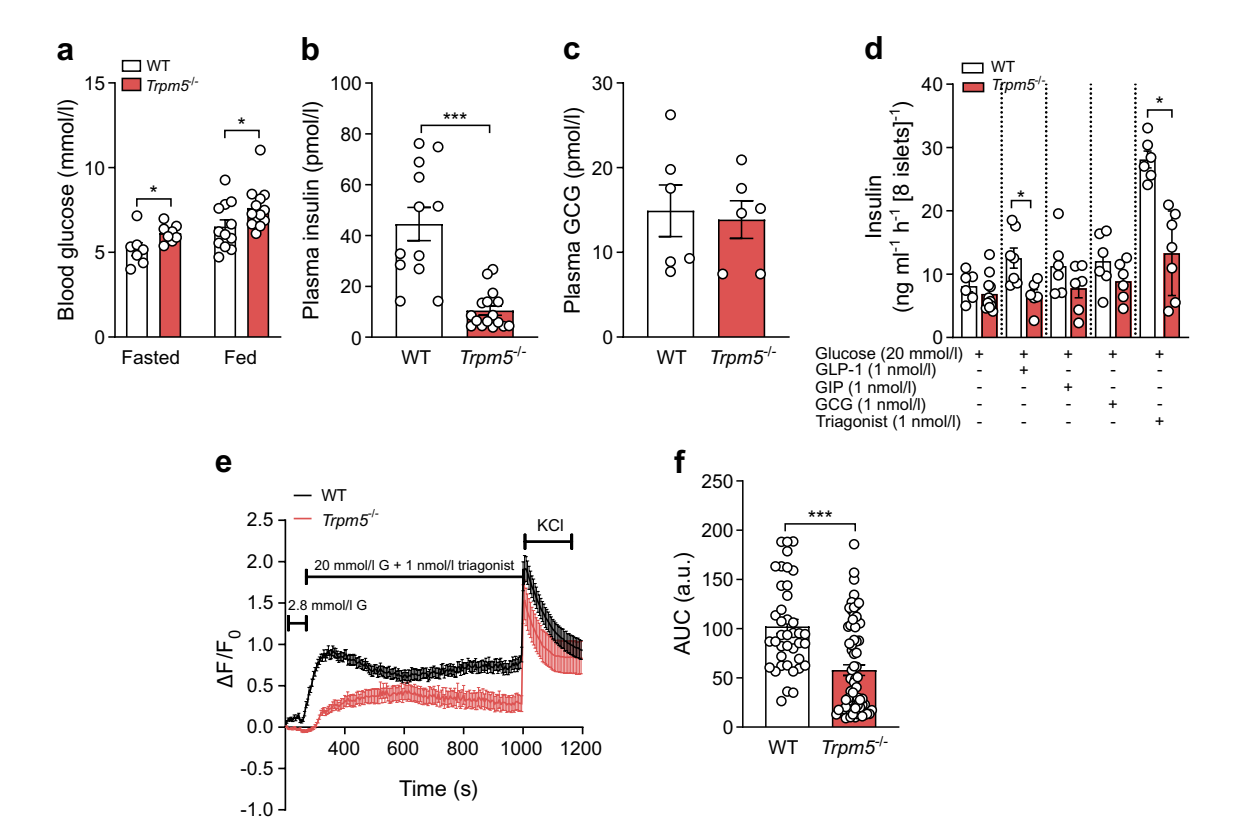


Fig. 6 Triagonist improves glycaemic management in a TRPM5-dependent manner. (a) Blood glucose (mmol/l) in fasted ($n \ge 7$ mice per genotype) or freely fed ($n \ge 12$ mice per genotype) mice. (b, c) Plasma insulin levels ($n \ge 12$ mice per genotype, b) and plasma GCG levels ($n \ge 6$ mice per genotype, c) in freely fed male and female $Trpm5^{-/-}$ mice and control littermates after 16 weeks of HFD and 3 weeks of treatment with triagonist. (d) Insulin secretion (ng ml⁻¹ h⁻¹ [8 islets]⁻¹) was assessed in isolated islets of $Trpm5^{-/-}$ and control littermate mice on HFD ($n \ge 5$ mice, measured in duplicate). After 1 h pre-incubation in KRB with 2.8 mmol/l glucose, islets were stimulated with 20 mmol/l glucose supplemented with mono- or multiagonist (1 nmol/l each). Insulin content was determined by ELISA in supernatant fractions collected 60 min after stimulation. (e) Intact WT mouse islets ($n \ge 40$ cells per condition, isolated from at least four

mice) and $Trpm5^{-/-}$ islets ($n \ge 30$ cells per condition, isolated from at least four mice) after 16 weeks of HFD and 3 weeks of treatment with triagonist were loaded with 3 µmol/l Fluo-4-AM and alterations in $[{\rm Ca}^{2+}]_i$ of individual cells were monitored by confocal microscopy after increasing the extracellular glucose concentration from 2.8 to 20 mmol/l in the presence of triagonist (1 nmol/l). KCl (30 mmol/l) was used as a positive control. F_0 was calculated as the mean fluorescence intensity during the final 2 min prior to stimulation with 20 mmol/l glucose + agonist. (f) AUC was assessed only during agonist application. The data are presented as means \pm SEM (circles in bar graphs represent single values) and statistical differences were assessed by unpaired two-tailed Student's t test (\mathbf{a} - \mathbf{c} , \mathbf{d} , \mathbf{f}). *p<0.05, ***p<0.001. a.u., arbitrary units; \mathbf{G} , glucose

Trpm5^{-/-} mice. The Trpm5^{-/-} mice exhibited slight glucose intolerance on LFD (Fig. 5a–c) and showed no significant changes in glucose tolerance after 16 weeks of HFD (Fig. 5d). The glucose-lowering effect of the triagonist observed in WT mice was significantly blunted in Trpm5^{-/-} mice after 16 weeks on HFD (Fig. 5e). Remarkably, triagonist-treated Trpm5^{-/-} mice showed significantly elevated fasting and fed blood glucose levels, accompanied by markedly reduced plasma insulin compared with their control littermates (Fig. 6a, b). The plasma levels of GCG remained comparable in both genotypes (Fig. 6c). Although the GSIS remained comparable in WT and Trpm5^{-/-} mouse islets, triagonist-induced GSIS was significantly reduced in Trpm5^{-/-} islets after 16 weeks on either LFD or HFD compared with controls (Fig. 6d and ESM Fig. 4). Importantly,

triagonist-induced initial Ca^{2+} peaks and elevations in intracellular Ca^{2+} levels were markedly reduced in $Trpm5^{-/-}$ mouse islets (Fig. 6e, f). Notably, only a slight impairment in glucose-induced Ca^{2+} responses was observed in $Trpm5^{-/-}$ mouse islets (ESM Fig. 5a–c). The islet morphology, beta to alpha cell ratio, and the islet size remained comparable in the $Trpm5^{-/-}$ mice and their control littermates (ESM Fig. 6a–c).

Discussion

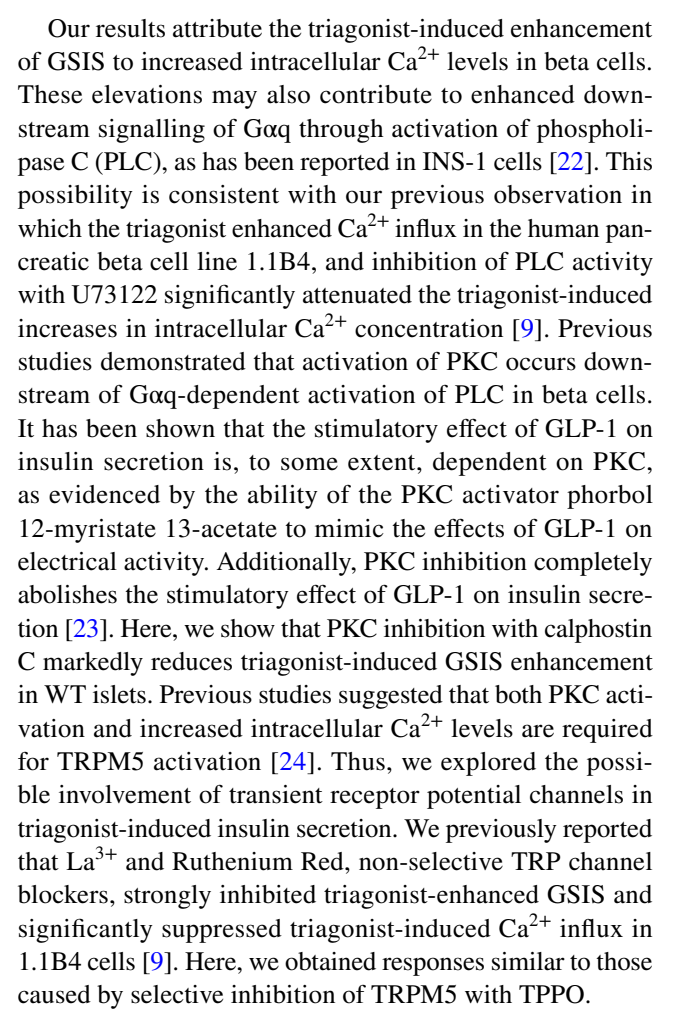
GLP-1, GIP and GCG are required to maintain normoglycaemic dynamics in healthy individuals. It is known that all three peptides enhance insulin secretion in WT mice,



through mechanisms likely involving G α s activation and cAMP production [19, 20]. However, a recent study demonstrated that in a mouse model of diabetes, GLP-1 exhibits preserved insulin secretion through a G α q-dependent manner [13]. The shift from G α s to G α q effective coupling in persistently depolarised beta cells may hint at therapeutic and pathophysiological significance.

The triagonist IUB447 has shown superior efficacy compared with existing dual co-agonists and best-in-class monoagonists in reducing body weight and improving glycaemic management in relevant rodent models. The enhanced insulin secretion induced by the triagonist is attributed to the simultaneous activation of all three receptors [1]. In the current study, we evaluated the significance of the GIPR and GCGR in triagonist-induced responses by employing $Gipr^{-/-}$ and $Gcgr^{-/-}$ mice. The results show that the triagonist functions independently of GIPR, as evidenced by fully intact triagonist enhancement of insulin secretion in Gipr^{-/-} mouse islets. The modest reduction in triagonist-induced insulin secretion observed in $Gcgr^{-/-}$ mouse islets was mirrored by comparable reductions in insulin secretion observed with other secretagogues. Although we initially attributed this to impaired beta cell function, as reported in $Gcgr^{-/-}$ mice [21], normalisation to protein content largely eliminated this effect. Additionally, pharmacological inhibition with LY2409021 indicated minimal involvement of GCGR in triagonist responses. Thus, we suggest that GIPR and GCGR are unlikely to be responsible for the enhanced effect of the triagonist on insulin secretion. These findings prompted us to hypothesise that GLP-1R may play a central role as the primary mediator of triagonist-induced responses in pancreatic islets. To test this, we employed a mouse model with a double Glp-1r and Gipr KO and a pharmacological approach using the specific GLP-1R antagonist exendin-3. Our data clearly demonstrate that the triagonist fails to enhance insulin secretion in the absence of functional GLP-1R activity. It is worth noting that the variability in agonist responses observed across different KO models may stem from differences in assay sensitivity, islet responsiveness and the physiological status of the mice, which can influence hormone responsiveness.

There is growing evidence indicating that GLP-1 activates both G α q and G α s signalling pathways, whereas the effects of GIP and GCG are mediated exclusively through G α s [13]. Here, we report that the triagonist IUB447 did not enhance cAMP accumulation in pancreatic islets and blocking of the adenylate cyclase had a minimal impact on triagonist-induced insulin secretion. However, inhibition of G α q signalling markedly suppressed the triagonist-induced enhancement of GSIS in WT mouse islets. A previous study showed that insulin secretion stimulated via the G α q signalling pathway is enhanced in persistently depolarised beta cells. The G α q agonist MK-2305 drastically improves glucose tolerance and insulin secretion in the KK-Ay mouse model of type 2 diabetes [13].



Modulation of TRPM5 activity plays a key role in regulating beta cell function and insulin secretion [25, 26]. TRPM5 SNPs are often associated with disrupted insulin secretion, elevated plasma glucose levels and lower GLP-1 levels [27]. Previous studies suggested that TRPM5 activation and the subsequent increases in Na⁺-influx play a crucial role in GLP-1-induced increases in beta cell electrical activity [28]. Although GLP-1 increases the amplitude of the voltage-gated Ca²⁺ current, closure of K_{ATP} channels is not the sole mechanism by which GLP-1 stimulates beta cell electrical activity. In both mouse and human beta cells, the ability of GLP-1 to induce membrane depolarisation and initiate action potential firing depend on extracellular Na⁺ and TRPM5 activity [23, 29, 30]. Importantly, the GLP-1-activated Na⁺ current cannot initiate electrical activity and insulin secretion unless the K_{ATP} channels are almost fully inhibited [23]. This is crucial for ensuring the safety of GLP-1-based drug therapy, as the stimulatory effect of such agents is glucose-dependent, and clarifies the rationale behind the minimal impact of the triagonist, even at significantly elevated concentrations, on insulin secretion under condition of low glucose.

In the current study, we showed that *Trpm5*^{-/-} mice fed HFD display glucose intolerance and impaired insulin



response to GLP-1. This finding is consistent with a previous study in which mice lacking TRPM5 function exhibited a decline in glucose tolerance and an impaired GSIS [31, 32]. Given our ex vivo findings that triagonist-induced insulin secretion is impaired by TRPM5 inhibition, we examined the effects of triagonist on glycaemic management in vivo in the absence of this channel. Here, we showed that triagonist treatment failed to reverse the impaired glucose tolerance in *Trpm5*^{-/-} mice. Furthermore, fasted and fed blood glucose levels were considerably higher in *Trpm5*^{-/-} mice than in their WT counterparts after triagonist treatment. This observation suggests the importance of TRPM5 function in mediating triagonist-induced increases in insulin secretion and overall normoglycaemia.

In this study, we report that the insulinotropic effect of the triagonist IUB447 is mainly due to its direct binding to the GLP-1R, leading to an increase in both Gαq signalling and TRPM5 activity. This observation agrees with our previously reported homology model, which indicated that the triagonist binds to the GLP-1R in the same binding pocket, in a very similar fashion to its native peptide agonist, GLP-1 [9]. A closer look into this model reveals several putative hydrogen bonds and a salt bridge that the triagonist forms in addition to those that are already present when GLP-1 binds in that pocket (see PDB ID 5VAI [33]). These additional bonds likely result in a stronger and longer binding of the triagonist to the GLP-1R when compared with GLP-1. These putative additional triagonist-specific bonds, beyond those that are identical to those formed when GLP-1 binds, include a possible salt bridge formation between Glu139 in the receptor and Arg23 of the triagonist (Gln23 in GLP-1) as well as hydrogen bonds between Arg190 in the receptor and Gln9 of the triagonist (Glu9 in GLP-1) and also between Arg121 in the receptor and Asp34 of the triagonist (Lys34 in GLP-1). Such a feature could affect the spatial adjustments of other elements during GLP-1R activation, potentially leading to improved therapeutic outcomes, as suggested by others [34]. Although our findings indicate that GLP-1R is the primary mediator of the insulinotropic effect of the triagonist in murine islets, receptor engagement may differ in human islets. Given that species-specific differences have been reported for other multi-agonists such as tirzepatide [35], further studies using human islets are warranted to confirm the involvement of GLP-1R and the Gαq-TRPM5 signalling axis in humans. Furthermore, it is important to note that our findings here specifically reflect the pharmacological profile of the triagonist IUB447, characterised by Finan et al. [1], and should not be extrapolated to structurally distinct triagonists such as SAR441255 [36] or LY3437943 [37], which may differ in receptor bias, potency and in vivo efficacy.

Supplementary Information The online version of this article (https://doi.org/10.1007/s00125-025-06525-0) contains peer-reviewed but unedited supplementary material.

Acknowledgements The authors specially thank B. Finan (Novo Nordisk Research Center Indianapolis, USA) and R. DiMarchi (Indiana University Bloomington, USA) for helpful discussion. The authors also thank A.-M. Postu (Bioinformatic, Munich, Germany) for the algorithms required for the data evaluation. We are also grateful for the technical assistance provided by fellow students T. Gentz and E. Cruz (MSc students, LMU Munich, Germany).

Data availability All data will be shared by the corresponding author upon reasonable request.

Funding Open Access funding enabled and organized by Projekt DEAL. NK and TG were supported by the Deutsche Forschungsgemeinschaft (German Research Foundation, DFG), — Project-ID 239283807 — TRR-152 (P23, P15). TDM received research funding from the German Research Foundation (DFG) within TRR-152 (P23) and TRR-296 and the German Center for Diabetes Research (DZD), and the European Union (ERC CoG) TRUSTED 101044445. ABeck was supported by the Deutsche Forschungsgemeinschaft (DFG) CRC 894 Project A14 and Forschungsausschuss der Universität des Saarlandes. ANeuberger is supported by the Elite Network of Bavaria, Bavarian State Ministry of Science and the Arts (Elitenetzwerk Bayern, Bayerisches Staatsministerium für Wissenschaft und Kunst). ANeuberger is also supported by WiFoMed (Verein zur Förderung von Wissenschaft und Forschung an der Medizinischen Fakultät der Ludwig-Maximilians-Universität München e.V.).

Authors' relationships and activities TDM receives funding from Novo Nordisk and has received speaking fees from Novo Nordisk, Eli Lilly, Boehringer Ingelheim, Merck, AstraZeneca, Mercodia and Berlin Chemie AG. TDM further holds stocks from Novo Nordisk and Eli Lilly. The authors declare that there are no other relationships or activities that might bias, or be perceived to bias, their work.

Contribution statement PCFS, PB, SB, ABeck, ABreit and ACS conducted experiments, analysed and interpreted data and edited the manuscript. PSR, ANovikoff, ANeuberger, TDM and IB interpreted data and edited the manuscript. TG directed the project, interpreted data and edited the manuscript. NK directed the project, designed and conducted experiments, analysed and interpreted data, prepared figures and wrote the manuscript. All authors approved the final version of the manuscript. NK is responsible for the integrity of the work as a whole.

Open Access This article is licensed under a Creative Commons Attribution 4.0 International License, which permits use, sharing, adaptation, distribution and reproduction in any medium or format, as long as you give appropriate credit to the original author(s) and the source, provide a link to the Creative Commons licence, and indicate if changes were made. The images or other third party material in this article are included in the article's Creative Commons licence, unless indicated otherwise in a credit line to the material. If material is not included in the article's Creative Commons licence and your intended use is not permitted by statutory regulation or exceeds the permitted use, you will need to obtain permission directly from the copyright holder. To view a copy of this licence, visit http://creativecommons.org/licenses/by/4.0/.

References

- Finan B, Yang B, Ottaway N et al (2015) A rationally designed monomeric peptide triagonist corrects obesity and diabetes in rodents. Nat Med 21(1):27–36. https://doi.org/10.1038/nm.3761
- Khajavi N, Biebermann H, Tschöp M, DiMarchi R (2017) Treatment of diabetes and obesity by rationally designed peptide



- agonists functioning at multiple metabolic receptors. Endocr Dev 32:165–182. https://doi.org/10.1159/000475737
- Müller TD, Finan B, Clemmensen C, DiMarchi RD, Tschöp MH (2017) The new biology and pharmacology of glucagon. Physiol Rev 97(2):721–766. https://doi.org/10.1152/physrev.00025.2016
- Svendsen B, Larsen O, Gabe MBN et al (2018) Insulin secretion depends on intra-islet glucagon signaling. Cell Rep 25(5):1127-1134.e1122. https://doi.org/10.1016/j.celrep.2018.10.018
- Heckemeyer CM, Barker J, Duckworth WC, Solomon SS (1983) Studies of the biological effect and degradation of glucagon in the rat perifused isolated adipose cell. Endocrinology 113(1):270–276. https://doi.org/10.1210/endo-113-1-270
- Day JW, Ottaway N, Patterson JT et al (2009) A new glucagon and GLP-1 co-agonist eliminates obesity in rodents. Nat Chem Biol 5(10):749–757. https://doi.org/10.1038/nchembio.209
- Zhang Q, Delessa CT, Augustin R et al (2021) The glucosedependent insulinotropic polypeptide (GIP) regulates body weight and food intake via CNS-GIPR signaling. Cell Metab 33(4):833-844.e835. https://doi.org/10.1016/j.cmet.2021.01.015
- 8. Borner T, Geisler CE, Fortin SM et al (2021) GIP receptor agonism attenuates GLP-1 receptor agonist-induced nausea and emesis in preclinical models. Diabetes 70(11):2545–2553. https://doi.org/10.2337/db21-0459
- 9. Khajavi N, Finan B, Kluth O et al (2018) An incretin-based tri-agonist promotes superior insulin secretion from murine pancreatic islets via PLC activation. Cell Signal 51:13–22. https://doi.org/10.1016/j.cellsig.2018.07.006
- Bavec A, Hällbrink M, Langel U, Zorko M (2003) Different role of intracellular loops of glucagon-like peptide-1 receptor in G-protein coupling. Regul Pept 111(1–3):137–144. https://doi.org/10. 1016/s0167-0115(02)00282-3
- Montrose-Rafizadeh C, Avdonin P, Garant MJ et al (1999) Pancreatic glucagon-like peptide-1 receptor couples to multiple G proteins and activates mitogen-activated protein kinase pathways in Chinese hamster ovary cells. Endocrinology 140(3):1132–1140. https://doi.org/10.1210/endo.140.3.6550
- Jia Y, Liu Y, Feng L, Sun S, Sun G (2022) Role of glucagon and its receptor in the pathogenesis of diabetes. Front Endocrinol 13:928016. https://doi.org/10.3389/fendo.2022.928016
- Oduori OS, Murao N, Shimomura K et al (2020) Gs/Gq signaling switch in β cells defines incretin effectiveness in diabetes. J Clin Investig 130(12):6639–6655. https://doi.org/10.1172/jci140046
- Lynn FC, Pamir N, Ng EH, McIntosh CH, Kieffer TJ, Pederson RA (2001) Defective glucose-dependent insulinotropic polypeptide receptor expression in diabetic fatty Zucker rats. Diabetes 50(5):1004–1011. https://doi.org/10.2337/diabetes.50.5.1004
- Xu G, Kaneto H, Laybutt DR et al (2007) Downregulation of GLP-1 and GIP receptor expression by hyperglycemia: possible contribution to impaired incretin effects in diabetes. Diabetes 56(6):1551–1558. https://doi.org/10.2337/db06-1033
- Khajavi N, Beck A, Riçku K et al (2023) TRPM7 kinase is required for insulin production and compensatory islet responses during obesity. JCI Insight 8(3):e163397. https://doi.org/10.1172/jci.insight.163397
- Khajavi N, Riçku K, Schreier PCF et al (2023) Chronic Mg(2+) deficiency does not impair insulin secretion in mice. Cells 12(13):1790. https://doi.org/10.3390/cells12131790
- Schindelin J, Arganda-Carreras I, Frise E et al (2012) Fiji: an open-source platform for biological-image analysis. Nat Methods 9(7):676–682. https://doi.org/10.1038/nmeth.2019
- Kashima Y, Miki T, Shibasaki T et al (2001) Critical role of cAMP-GEFII–Rim2 complex in incretin-potentiated insulin secretion. J Biol Chem 276(49):46046–46053. https://doi.org/10.1074/ jbc.M108378200
- Seino S, Shibasaki T (2005) PKA-dependent and PKA-independent pathways for cAMP-regulated exocytosis. Physiol Rev 85(4):1303–1342. https://doi.org/10.1152/physrev.00001.2005

- Sørensen H, Winzell MS, Brand CL et al (2006) Glucagon receptor knockout mice display increased insulin sensitivity and impaired beta-cell function. Diabetes 55(12):3463–3469. https:// doi.org/10.2337/db06-0307
- Thore S, Dyachok O, Tengholm A (2004) Oscillations of phospholipase C activity triggered by depolarization and Ca2+ influx in insulin-secreting cells. J Biol Chem 279(19):19396–19400. https://doi.org/10.1074/jbc.C400088200
- Shigeto M, Ramracheya R, Tarasov AI et al (2015) GLP-1 stimulates insulin secretion by PKC-dependent TRPM4 and TRPM5 activation. J Clin Investig 125(12):4714

 4728. https://doi.org/10.1172/jci81975
- Liman ER (2007) TRPM5 and taste transduction. Handb Exp Pharmacol 179:287–298. https://doi.org/10.1007/978-3-540-34891-7 17
- Philippaert K, Pironet A, Mesuere M et al (2017) Steviol glycosides enhance pancreatic beta-cell function and taste sensation by potentiation of TRPM5 channel activity. Nat Commun 8:14733. https://doi.org/10.1038/ncomms14733
- Vennekens R, Mesuere M, Philippaert K (2018) TRPM5 in the battle against diabetes and obesity. Acta Physiol (Oxford, England) 222(2). https://doi.org/10.1111/apha.12949
- 27. Ketterer C, Müssig K, Heni M et al (2011) Genetic variation within the TRPM5 locus associates with prediabetic phenotypes in subjects at increased risk for type 2 diabetes. Metab Clin Exp 60(9):1325–1333. https://doi.org/10.1016/j.metabol.2011.02.002
- 28. Prawitt D, Monteilh-Zoller MK, Brixel L et al (2003) TRPM5 is a transient Ca2+-activated cation channel responding to rapid changes in [Ca2+]i. Proc Natl Acad Sci U S A 100(25):15166–15171. https://doi.org/10.1073/pnas.2334624100
- Fridolf T, Ahrén B (1991) GLP-1(7–36) amide-stimulated insulin secretion in rat islets is sodium-dependent. Biochem Biophys Res Commun 179(1):701–706. https://doi.org/10.1016/0006-291x(91)91429-g
- 30. Kato M, Ma HT, Tatemoto K (1996) GLP-1 depolarizes the rat pancreatic beta cell in a Na(+)-dependent manner. Reg Pept 62(1):23–27. https://doi.org/10.1016/0167-0115(95)00164-6
- Colsoul B, Schraenen A, Lemaire K et al (2010) Loss of high-frequency glucose-induced Ca2+ oscillations in pancreatic islets correlates with impaired glucose tolerance in Trpm5-/- mice. Proc Natl Acad Sci U S A 107(11):5208–5213. https://doi.org/10.1073/pnas.0913107107
- Brixel LR, Monteilh-Zoller MK, Ingenbrandt CS et al (2010) TRPM5 regulates glucose-stimulated insulin secretion. Pflugers Arch Eur J Physiol 460(1):69–76. https://doi.org/10.1007/ s00424-010-0835-z
- Zhang Y, Sun B, Feng D et al (2017) Cryo-EM structure of the activated GLP-1 receptor in complex with a G protein. Nature 546(7657):248–253. https://doi.org/10.1038/nature22394
- Liang YL, Khoshouei M, Glukhova A et al (2018) Phase-plate cryo-EM structure of a biased agonist-bound human GLP-1 receptor-Gs complex. Nature 555(7694):121–125. https://doi.org/10. 1038/nature25773
- El K, Douros JD, Willard FS et al (2023) The incretin co-agonist tirzepatide requires GIPR for hormone secretion from human islets. Nat Metab 5(6):945–954. https://doi.org/10.1038/s42255-023-00811-0
- 36. Bossart M, Wagner M, Elvert R et al (2022) Effects on weight loss and glycemic control with SAR441255, a potent unimolecular peptide GLP-1/GIP/GCG receptor triagonist. Cell Metab 34(1):59-74.e10. https://doi.org/10.1016/j.cmet.2021.12.005
- Coskun T, Urva S, Roell WC et al (2022) LY3437943, a novel triple glucagon, GIP, and GLP-1 receptor agonist for glycemic control and weight loss: From discovery to clinical proof of concept. Cell Metab 34(9):1234-1247.e1239. https://doi.org/10.1016/j.cmet.2022.07.013

Publisher's Note Springer Nature remains neutral with regard to jurisdictional claims in published maps and institutional affiliations.

